

# Characterizing the ac-dc-ac Degradation of Aircraft and Vehicle Organic Coatings using Embedded Electrodes

Gordon P. Bierwagen<sup>†</sup>, Kerry N. Allahar, Quan Su, and Victoria Johnston-Gelling

Department of Coatings and Polymeric Materials, North Dakota State University, Fargo, ND 58105 USA

Embedded sensors were used as an in-situ corrosion-sensing device for aircraft and vehicular structures protected by organic coatings. Results are presented changes associated with a standard Airforce aircraft coating and a standard Army vehicle coating were monitored by embedded sensors. These coatings consisted of a polyurethane topcoat and an epoxy primer, however are formulated to provide different characteristics. The ac-dc-ac testing method was used to accelerate the degradation of these coatings while being immersed in a NaCl medium. Electrochemical impedance spectroscopy and electrochemical noise measurement experiments were used to monitor the induced changes. A comparison of the results between coatings subjected to the ac-dc-ac exposure and coatings subjected to only constant immersion in the NaCl medium is presented. The results were used to demonstrate the effectiveness of the ac-dc-ac method at accelerating the degradation of an organic coating without observably changing the normal mechanism of degradation. The data highlights the different features of the coating systems and tracks them while the coating is being degraded. The aircraft coating was characterized by a high-resistant topcoat that can mask corrosion/primer degradation at the primer/substrate interface whereas the vehicle coating was characterized by a low-resistant topcoat with an effective corrosion inhibiting primer. Details of the ac-dc-ac degradation were evaluated by using an equivalent circuit to help interpret the electrochemical impedance data.

**Keywords:** electrochemical impedance spectroscopy, electrochemical noise method, ac-dc-ac testing, equivalent circuit modeling

## 1. Introduction

The primary means of corrosion protection for industrial metallic structures is an organic barrier coating which reduces the transport of water and entrained ionic species to the substrate. There has been development of practical sensing techniques that monitor *in situ* the barrier effect of a coating that are based on the electrochemical properties of the coating by placing a sensor on the top of the coating system.<sup>1),2),3),4),5),6)</sup> More effective sensors that can be used to diagnose effects within the coatings system layers are the embedded electrode sensors.<sup>1),2),3),4),5)</sup> A technique for *in situ* monitoring of a coating with a.c. involves the application of an embedded electrode or sensor within the coating.<sup>8),9),10),11)</sup> Kittel *et al.* reported electrochemical impedance spectroscopy EIS results associated with the topcoat and basecoat of a coating system using gold and nickel sensors embedded between two layers of the same coating type.<sup>9),10)</sup> The effect of moisture on the interlayer adhesion between a topcoat and a basecoat was evaluated

by Miszczyk and Schauer using embedded electroconductive ink sensors between the coats.<sup>11)</sup> A recent report by Allahar *et al.*, included data that demonstrated that the presence of embedded electrodes on the performance of the coating system was not significant.<sup>1)</sup>

Embedded electrodes have also been used to acquire electrochemical noise measurement ENM associated with coated AA 2024-T3.<sup>8),13)</sup> Reported results indicated that lower noise resistance and spectral noise resistance parameter values were associated with higher environmental humidity and increased aging.<sup>8)</sup> Thermal cycling is an accelerated bench-top experiment that have been used to qualify and rank coating performances in weeks as opposed to years. This method was used to test standard Air Force coatings with sensors.<sup>13)</sup> The EIS and ENM results presented indicated that the sensors were able to monitor the basecoat-substrate system more closely as compared to a conventional 3E configuration with a RE located exterior to the coating.

Another accelerated bench top experiment used for ranking coating performance is the ac-dc-ac test that was introduced by Hollaender *et al.*<sup>1)</sup> In this test changes in-

<sup>†</sup> Corresponding author: Gordon.Bierwagen@ndsu.edu

duced by an imposed constant cathodic polarization d.c. are monitored by an EIS experiment with a rest period allowing equilibrium between the coating and the electrolyte to be restored.<sup>14),1),2),3),4)</sup> The coating degradation associated with this test includes the deterioration of the coating itself due to formation of preferred pathways for water and electrolyte transport. the delamination of the coating from the substrate due to the production of hydroxide ions from the hydrogen evolution that is promoted by the cathodic d.c., and the increase in the ionic species in the coating due to the influx promoted by the ionic current during the d.c. cathodic polarization. The application of the ac-dc-ac technique as an accelerated testing technique for coatings with sensors is presented here for the first time. The results for the Air Force and Army coatings investigated indicated the performance of the coating layers and that this test method can be used to degrade these coatings in a reproducible way. Much of the barrier resistance is provided by the primer and the primer/substrate interface and can be adequately monitored by the sensors.

## 2. Experiment

Embedded sensors were used to investigate the influence of the ac-dc-ac test condition on standard Air Force aircraft and Army vehicle coatings. The Air Force coating system consisted of an Deft 02-Y-40 epoxy primer (60  $\mu\text{m}$ ) and a Deft 03-GY-277 (50  $\mu\text{m}$ ) urethane topcoat. The Army vehicle coating systems consisted of a MIL-P-53022B Type II epoxy primer (80  $\mu\text{m}$ ) and a MIL-DIL-64159 Type II urethane topcoat (50  $\mu\text{m}$ ). These coatings are referred to as AF and AM coatings, respectively, in this paper. Steel substrates used in the experiments were supplied by the Army and the AA 2024-T3 substrate for the AF coatings was supplied by Q-panel. Pt embedded electrodes were used which were less than 1 micron thick and were supplied by Wrights of Lymm Ltd., Manchester, England. The embedded sensor was consisted of two rectangular strips, 28 mm by 4 mm each, connected by a 12 mm by 4 mm strip at one end.

### 2.1 Panel Preparation

Pretreatment of the AM steel panels included sanding to 200 grit followed by 800 grit, then washing with hexane. The AF panels were used as received (mill finished) and pretreatment included washing with hexane followed by washing with a phosphoric/alcohol solution. The panels were coated immediately after they had been pretreated. The primers and topcoats were applied using a regular air spray gun in accordance with the standard application procedure provided by the manufacturers. The primer was

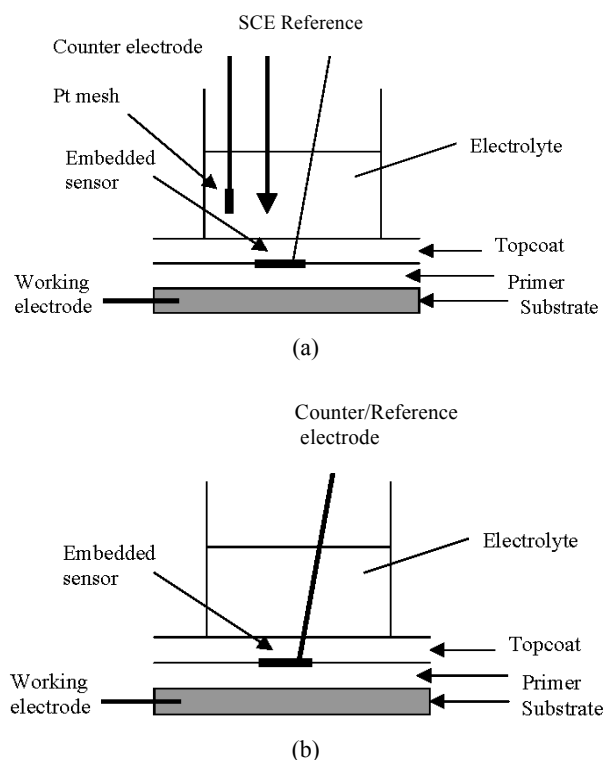


**Fig. 1.** Schematic diagrams of the EIS measurement configuration associated with (a) the three electrode configuration and (b) the two-electrode configuration.

cured at room temperature for three days in a hood before the topcoat application and the topcoat similarly cured. An Elcometer 345 NS, supplied by Elcometer Instruments Ltd. of Rochester Hills, MI, was used for measuring the coating thickness.

Support for the delicate Pt leaves was obtained by securing them unto a plastic transparency film by a weak emulsion adhesive. The supported leaves were then cut into the desired shape of the sensor as shown in Fig. 1. The surface area of the sensor was 5.28  $\text{cm}^2$ . The application of the sensor involved attaching the platinum side to the cured primer surface using a homemade epoxy adhesive. The supporting transparency film was peeled off with the platinum sensor adhered to the primer after the adhesive was dry. Electrical connection to the sensor was achieved by soldering a copper core wire onto the sensor and sealing the joint with an epoxy resin that was allowed to harden at room temperature for one day before the application of the topcoat.

### 2.2 ac-dc-ac Testing Method

The ac-dc-ac testing method<sup>14),18)</sup> as it is used in this study involves immersing the areas of the coated panels in 3.5 wt. % NaCl solution while performing three steps

of a cyclic procedure. The steps were an a.c. step where the electrochemical properties of the coating were monitored using EIS and ENM, a d.c.-step where an applied cathodic potential was applied to promote the hydrogen evolution reaction and ionic current flow through the coating and a rest step where the processes that were accelerated due to the applied potential were allowed to relax.

Four samples of Air Force coating and Army coating systems were used. Two samples of each coating system were exposed to the ac-dc-ac testing. These samples were identified as AF1 and AF2, and AM1 and AM2 for the Air Force and Army coating systems, respectively. Two samples of each coating system were used as controls where the samples were only immersed without ac-dc ac testing. These samples were identified as CAF1 and CAF2, and CAM1 and CAM2 for the Air Force and Army coating systems, respectively.

The testing procedure for the samples exposed to the ac-dc-ac testing included an initial 20 day period in which no d.c. was applied. This was to allow the samples to be equilibrated with the immersing electrolyte. Following the 20 days, each day the samples were monitored using EIS and ENM and then exposed to one cycle of d.c. potential for a specified application time. After the d.c. potential the samples were allowed to return to equilibrium overnight.

The d.c. potentials used for the ac-dc-ac testing of the Air Force coating were  $-2$  V and  $-4$  V. The  $-2$  V potential were used for the first 70 cycles with application times of 0.5 hour (cycles 1 to 43), 1 hour (cycles 44 to 53) and 2 hours (cycles 54 to 70). The  $-4$  V potential was applied for the following 20 cycles with application times of 2 hours (cycles 71 to 80) and 4 hours (cycles 81 to 90).

The d.c. potentials used for the Army coatings were  $-2$  V,  $-4$  V and  $-8$  V. The  $-2$  V potential were used for the first 60 cycles with application times of 0.5 hour (cycles 1 to 40), 1 hour (cycles 41 to 50), 2 hour (cycles 51-60). The  $-4$  V potential was used for the next 10 cycles with an application time of 2 hour. The  $-8$  V potential was used for the following 13 cycles with application times of 2 hour (cycles 71 to 80) and 8 hours (cycles 81 to 83).

The EIS and ENM electrochemical experiments were performed using a Gamry PCI4/300 TM system in conjunction with the software Gamry Framework Version 4.21/EIS 300 and Gamry Framework Version 4.21/ESA 400 software. A frequency range from 10 kHz to 10 mHz and a perturbation amplitude of 10 mV were used for the potentiostatic EIS measurements included with the a 10 points per decade data acquisition rate. The ENM measure-

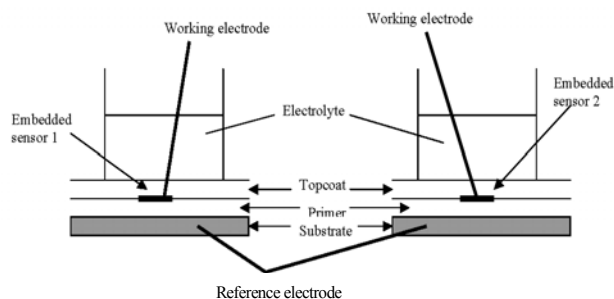


**Fig. 2.** Schematic diagram of the experimental setup for an ENM measurement associated with the sensors on two panels. The substrates are connected as the reference electrode and the embedded sensors from the samples are the two working electrodes.

ment frequency was 10 Hz and 254 points per block with 10 blocks per panel pair. The d.c. steps were performed using Gamry Framework Version 4.21/DC 105 software. The test cell consisted of the coated substrate with a perspex cylinder/O-ring seal clamped on.<sup>14)</sup> The surface area of the coated substrates was  $7.07 \text{ cm}^2$ .

### 2.3 Experimental Configurations

EIS measurements on the topcoat/primer/substrate systems were performed using a three-electrode (3E) configuration where a standard calomel electrode (SCE) was the RE, a platinum mesh was the counter electrode (CE) and the substrate was the working electrode (WE) (see Fig. 1a). EIS measurements on the primer/substrate system were performed using a two-electrode (2E) configuration where the sensor was the RE/CE and the substrate was the WE (see Fig 1b).

The configuration for the ENM experiment is shown in Fig. 2 and consisted of the two sensors as WEs and the electrically connected substrates as the CE. The application of the d.c. step of the ac-dc-ac testing method for the 2-panel setup comprised of applying the dc between electrically connected sensors and electrically connected substrates.

### 3. Results and Discussion

The results presented for the coatings as functions of the immersion time include the open circuit potential, the low frequency modulus, the capacitance and the noise resistance parameter. A measure of the barrier properties of a coating is the resistance associated with a low frequency.<sup>12),13)</sup> A frequency of 0.1 Hz was selected for the low frequency modulus. The notation  $|Z|_{in}$  was used for the impedance data associated with the sensor measurement of the primer/substrate system and the notation  $|Z|_{total}$

was used for the impedance data associated with the top-coat/primer/substrate system. The spectra associated with the inner systems were analyzed using an equivalent circuit.

### 3.1 Low Frequency Modulus

The low frequency modulus of single layered coatings represents the net resistance of the bulk coating, the coating/substrate interface and the charge transfer resistance of the metallic substrate. The low frequency modulus for two layered coatings represents the net resistance of the bulk topcoat, the topcoat-basecoat interlayer, the bulk basecoat, the basecoat/substrate interface and the charge transfer resistance of the substrate.<sup>13)</sup> The charge transfer resistance is the resistance that determines the corrosion rate at the substrate, and most often this is the resistance

that is associated with the low frequency modulus of EIS data.

The  $|Z|_{\text{total}}$  and  $|Z|_{\text{in}}$  values for the Air Force coatings are shown in Figs. 3a and 3b, respectively. The  $|Z|_{\text{total}}$  values of CAF1 and CAF2 decreased by 1 order of magnitude over the initial 20 day immersion. The values of  $|Z|_{\text{in}}$  for the tested and control coatings decreased by up to two orders of magnitude during the initial 20 day immersion. This indicated that the four coating systems, as measured by the sensors, were similar. There was little change associated with the control coatings CAF1 and CAF2, with  $|Z|_{\text{total}}$  values of approximately  $10^9 \Omega \text{ cm}^2$  and  $10^8 \Omega \text{ cm}^2$  for the 110 day immersion, respectively and  $|Z|_{\text{in}}$  values of approximately  $10^7 \Omega \text{ cm}^2$  for both CAF1 and CAF2. The significantly larger value of the  $|Z|_{\text{total}}$  as compared to  $|Z|_{\text{in}}$  for the AF coatings indicated that the topcoat was providing the dominant part of the total protection provided by the multilayer system. There was a change in the  $|Z|_{\text{total}}$  and  $|Z|_{\text{in}}$  values for the coatings AF1 and AF2 under ac-dc-ac test protocol during the  $-2 \text{ V}$  d.c. cycles. Upon the application of the  $-4 \text{ V}$  d.c. cycles both the  $|Z|_{\text{total}}$  and  $|Z|_{\text{in}}$  values associated with AF1 and AF2 decreased with each cycle. The d.c. induced decrease of  $|Z|_{\text{in}}$  can be attributed to the delamination at the metal coating interface while the decrease in the  $|Z|_{\text{in}}$  value can be attributed to the degradation of the topcoat coupled with the coating delamination.

The  $|Z|_{\text{total}}$  and  $|Z|_{\text{in}}$  values for the Army coatings are shown in Figs. 4a and 4b, respectively. The  $|Z|_{\text{total}}$  and  $|Z|_{\text{in}}$  values associated with the samples tested AM1 and AM2, and the control samples, CAM1 and CAM2 were approximately  $10^9 \Omega \text{ cm}^2$  for the immersion time up to 101 days. A decrease in the values for CAM1 was observed at 70 days but the values recovered by the 80th day of immersion. These results which indicated that the Army vehicle topcoat was not as significant a contributor to the total protection of the Army multicoat system as was the primer. The 102nd day values for AM2 of  $|Z|_{\text{total}}$  and  $|Z|_{\text{in}}$  dropped off significantly by 1 order of magnitude demonstrating that the  $-8 \text{ V}$  d.c. 8 hour test condition induced deterioration of the Army vehicle coating.

Comparison of the measured values of  $|Z|_{\text{in}}$  and  $|Z|_{\text{total}}$  indicated that the most significant contributor to the barrier properties of the Army coating was the primer/substrate interlayer and not the topcoat, whereas for the Air Force coating, the most important contributor was the topcoat. The measurement of  $|Z|_{\text{in}}$  provided by the sensors in the coatings monitored the changes associated with the primer/substrate. The consistency among the four sensors for the Army and Air Force coatings demonstrated the reliability of the sensors as *in situ* monitoring devices in iden-

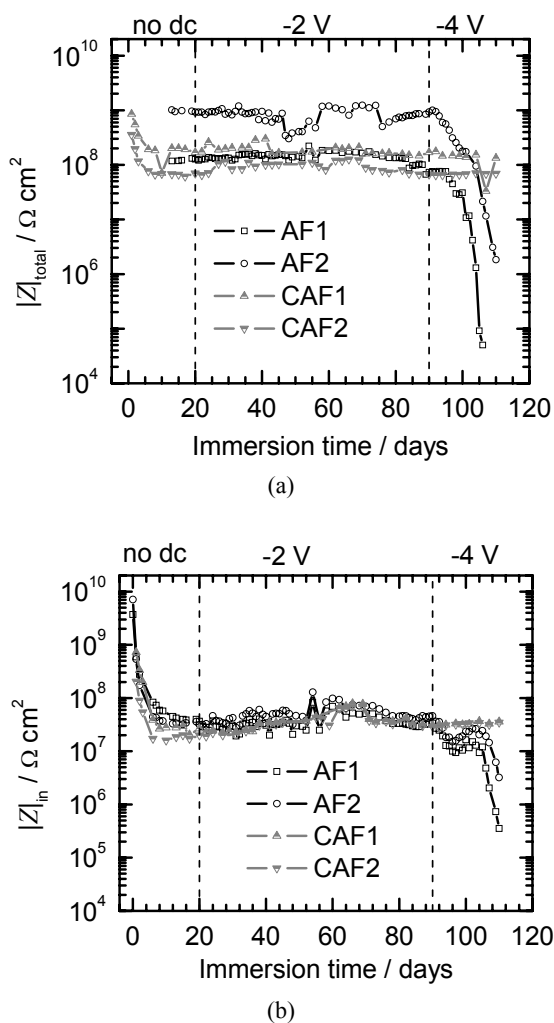


**Fig. 3.** Low frequency modulus as a function of immersion time under the ac-dc-ac test protocol for EIS measurements made for (a)  $|Z|_{\text{total}}$  and (b)  $|Z|_{\text{in}}$  of the EIS data associated with the Air Force coatings.

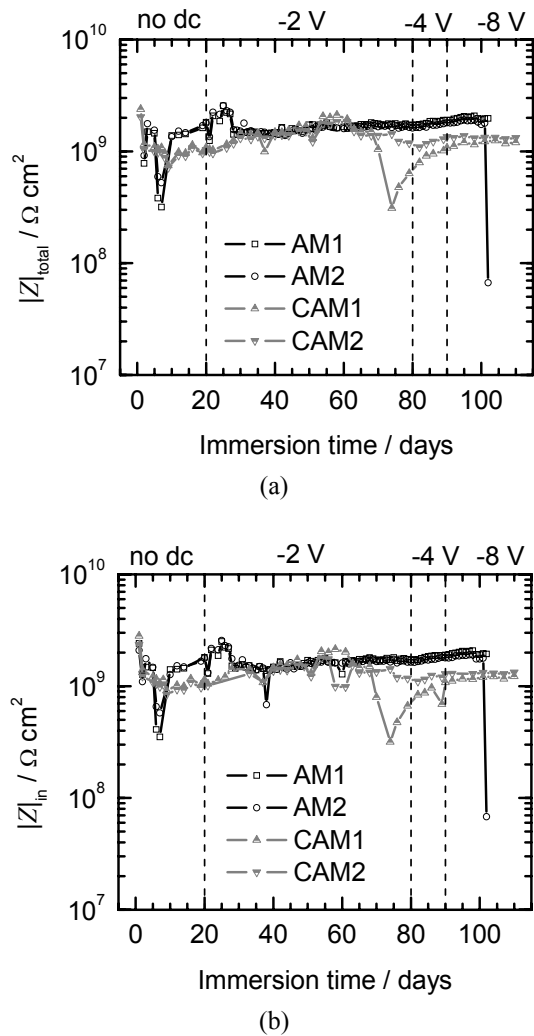


**Fig. 4.** Low frequency modulus as a function of immersion time under the ac-dc-ac test protocol for EIS measurements made for (a)  $|Z|_{total}$  and (b)  $|Z|_{in}$  in the EIS data associated with the Army coatings.

tifying contributions of the individual coating layers and interlayers.

The low frequency modulus data presented in Figs. 4 and 5 indicated that the Army coating system performed better than the Air Force coating system under the ac-dc-ac testing conditions. These results demonstrated the usefulness of the ac-dc-ac test for ranking coatings in time periods of weeks as opposed to months.

### 3.2 Equivalent Circuit Modeling

A schematic diagram of a coated substrate is shown in Fig. 5(a) where the two-coat system is divided into the bulk topcoat, topcoat-primer interlayer, bulk primer coat, and the adhesion region.<sup>14)</sup> The adhesion region represents an interlayer that is immediately adjacent to the substrate

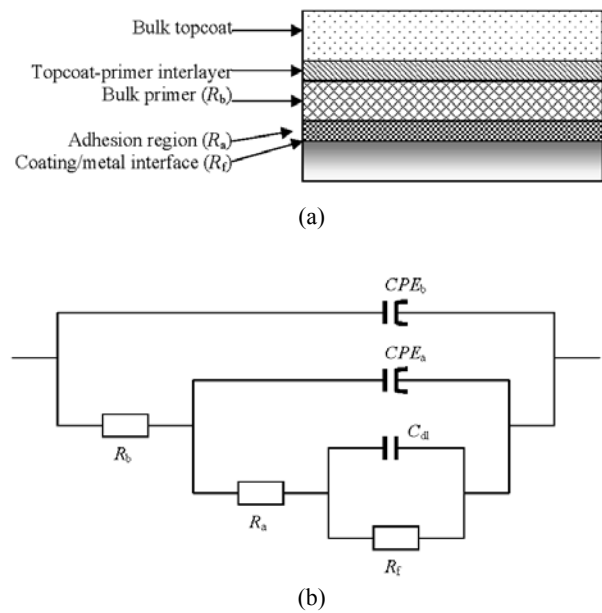
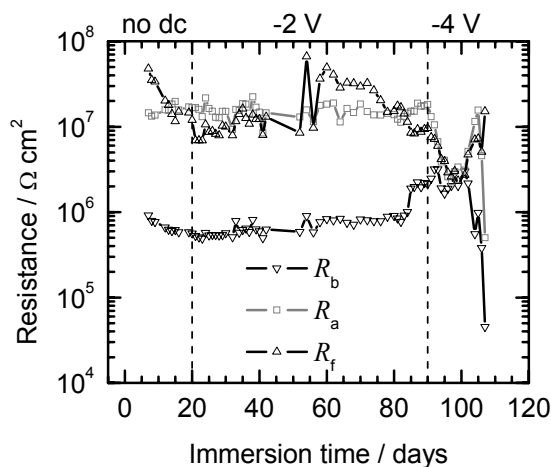


**Fig. 5.** Schematic diagrams of (a) coating-substrate separated into layers and (b) equivalent circuit used for fitting EIS data.

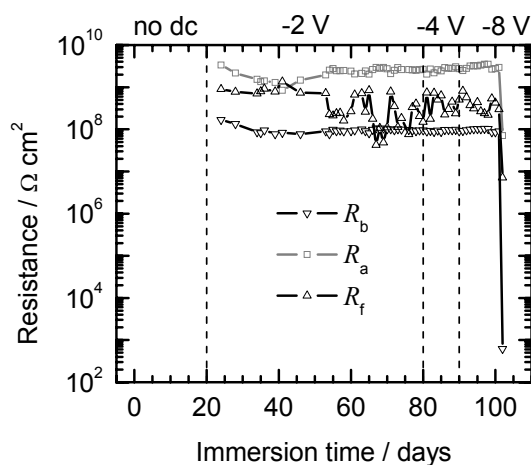
but distinct from the bulk primer.<sup>10)</sup> The properties of polymers are altered in the interphase region by restrictions in the configurations that the polymer molecules can take due to adsorption, and this region has measurably distinct properties from the bulk polymer.<sup>1),2)</sup> The equivalent circuit shown in Fig. 5(b) was used to analyze the EIS data associated with the measurements from the sensors. This circuit addressed the resistance of the bulk primer and adhesion region layers, and the charge transfer resistance. The circuit parameters  $CPE_b$  and  $CPE_a$  were assumed to represent the constant phase element (CPE) behavior of the bulk of the primer and adhesion region, respectively. The parameters  $R_b$  and  $R_a$  were assumed to represent the resistance behavior of the bulk primer [subscript b in Fig. 5.(b)] and adhesion region (subscript a) of the primer/substrate interface, respectively. The parameters  $C_{dl}$  and  $R_f$  were assumed to represent the double layer capacitance and the charge transfer resistance at the primer-substrate interface (subscript f), respectively. A Fortran program written with Compaq Visual Fortran version 6.5.0. was used to perform the regression of the equivalent circuit model of Fig. 5(b) to the EIS data. The program employed a nonlinear least squares fitting using a modified simplex minimization method.<sup>1)</sup> The performance of this program was benchmarked with the commercial software *ZsimpWin* version 2.00 supplied by Echem Software of Ann Arbor, MI, USA.

Regressed parameter values for the EIS sensor data of CAF2 were  $10^7$ ,  $10^7$ , and  $10^6$   $\Omega\text{-cm}^2$  for  $R_f$ ,  $R_a$ , and  $R_b$ ,

respectively. The resistance parameters as functions of immersion time are shown in Fig. 6(a) for the EIS data associated with the sensor measurement for AF2. The values of  $R_f$  and  $R_a$  ranged between  $10^7$  and  $10^8 \Omega\text{-cm}^2$  up to 80 days of immersion. The  $R_b$  value was approximately  $10^6$  for the first 80 days of immersion. These results were consistent with the results associated with CAF2 and indicated that the Air Force coating was resistant to up to 60 cycles of the  $-2$  V d.c. condition. Immersion times of 91 to 100 days and over 100 days included d.c. conditions of  $-2$  V and  $-4$  V, respectively. There were changes in the parameters observed for the period between 90 and 110 days with a significant decrease in  $R_b$  and  $R_a$  and no change in  $R_f$  being observed. The unchanging charge-transfer resistance parameter  $R_f$  indicated that the



(a)



(b)

**Fig. 6.** Coating resistance parameters for the equivalent circuit model as a function of immersion time for EIS measurements made using the sensor for (a) the Air Force coating AF2 and (b) the Army coating AM2.

ac-dc-ac testing protocol used were not able to degrade the anti-corrosion properties of the Air Force coating system. The adhesion region resistance parameter was similar to the  $R_f$  parameter in magnitude until it dropped off after 90 days of immersion. The adhesion layer resistance may be a measure of the coating metal adhesion and the decrease in its value under the  $-4$  V d.c. condition indicated that this imposed potential was inducing delamination. The value of  $10^6 \Omega\text{-cm}^2$  for  $R_b$  when compared with the  $10^7 \Omega\text{-cm}^2$  value of  $R_a$  and  $R_f$  supported the conclusion that a significant resistance/barrier contributor of the Air Force coating primer was located at the coating/substrate interface.

Regressed parameter values for the EIS sensor data of CAM2 were  $10^9$ ,  $10^9$ , and  $10^8 \Omega\text{-cm}^2$  for  $R_f$ ,  $R_a$ , and  $R_b$ , respectively. The resistance parameters as functions of immersion time are shown in Fig. 6(b) for the EIS data associated with the sensor measurement for AM2. The values of  $R_a$ , and  $R_b$  were approximately  $10^8$ , and  $10^9 \Omega\text{-cm}^2$ , respectively, for up to 101 days of immersion. The values for  $R_f$  oscillated in the  $10^8$  and  $10^9 \Omega\text{-cm}^2$  range. During this time the coating was subjected to 60 cycles of  $-2$  V d.c., 10 cycles of  $-4$  V d.c., and 10 cycles of  $-8$  V d.c. (2 hours). The values of the three parameters decreased significantly at the 102<sup>nd</sup> day immersion after being subjected to  $-8$  V d.c. for 8 hours. These results indicated that the Army vehicle primer was not deteriorated at the  $-4$  V d.c. potential but was affected by the  $-8$  V d.c. condition. The consequent large decrease in the bulk primer resistance suggested that the bulk primer barrier properties are insignificant to the performance of the Army coating system and easily degraded by exposure.

The analysis of the EIS data using the equivalent circuit model of Fig. 5(b) provided a more detailed examination of the barrier characteristics of the primer/substrate systems. The essential driving force for the deterioration as determined from the low frequency data and the equivalent circuit model data was the applied cathodic potential. The value of the cathodic current as a function of immersion time is shown in Fig. 8 for the Air Force and Army coating systems. The Air Force coating current was approximately  $10^{-7} \text{ A cm}^2$  for the  $-2$  V condition but increased with each cycle upon the application of the  $-4$  V condition. Correlation of the data in Figs. 6(a) and 7(a) suggested that the increase in current for the  $-4$  V condition did not manifest changes in the  $R_f$  parameter although there were changes induced in the  $R_b$  and  $R_a$  parameters. An explanation for this was that the anti-corrosion properties of the Air Force primer were recovered when the imposed  $-4$  V potential was removed and the coating was allowed to return to its open circuit potential.

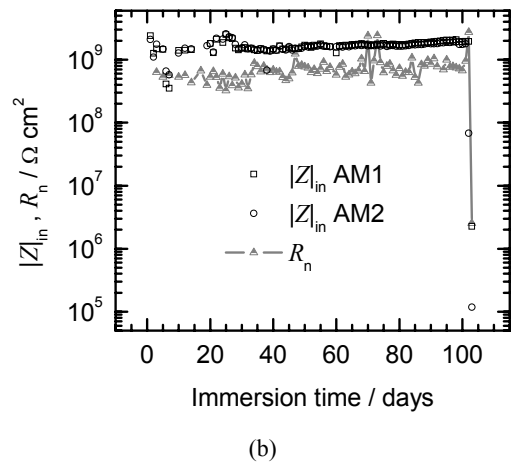
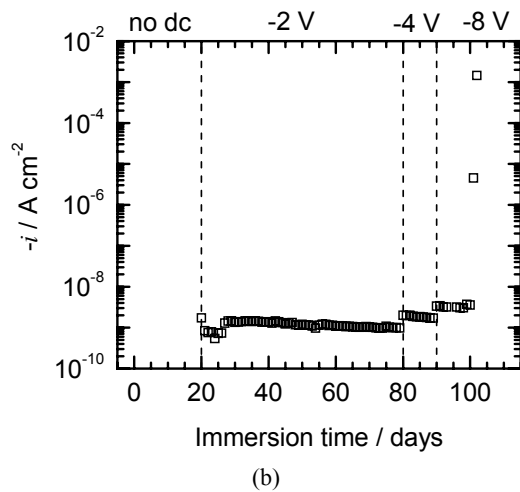
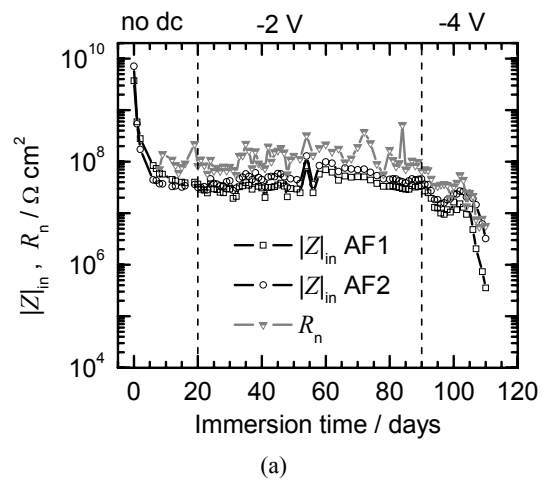
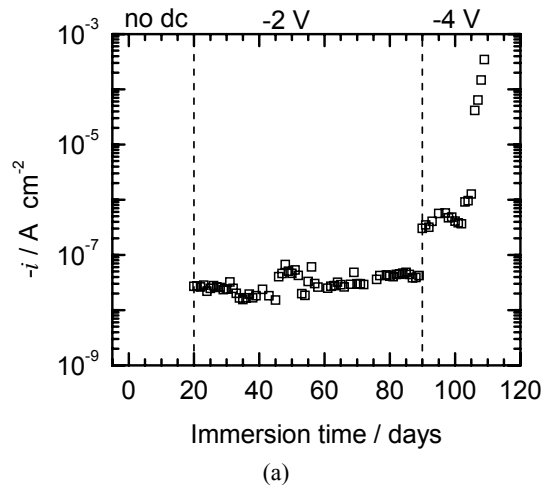


**Fig. 7.** Induced cathodic current density occurring during the dc portion of the ac-dc-ac protocol as a function of immersion time for (a) Air Force and (b) Army coatings.

**Fig. 8.** Coating resistance parameters  $R_n$  and  $|Z|_{in}$  as functions of immersion time for (a) the Air Force coatings and (b) the Army coatings.

The Army primer behaved differently as seen in the correlation of the data in Figs. 6(b) and 7(b). The  $-2$  V,  $-4$  V and  $-8$  V (2 hours) conditions did not induce changes in the coating, with the current values being less than  $10^{-8}$  A  $cm^2$ . The  $-8$  V (8 hours) condition however resulted in a large current that induced changes in the  $R_i$ ,  $R_a$ , and  $R_b$  parameters. The large decrease in the last parameter suggesting that the barrier protection of the system had been breached and irreversible damage had occurred.

### 3.3 Electrochemical Noise Measurements

The noise resistance  $R_n$  values are given as functions of immersion time in Fig. 8(a) for the Air Force coatings exposed to the ac-dc-ac testing. Included in this Fig. are the values of  $|Z|_{in}$  associated with the two coatings. The trend observed for the  $|Z|_{in}$  and  $R_n$  values were similar. The value of  $R_n$  decreased over the initial 20 day im-

ersion when no d.c. potential was applied. It remained approximately  $10^8$   $\Omega\text{-cm}^2$  for up to 80 days on immersion after which it decreased monotonically with immersion time. The decrease was more pronounced when the  $-4$  V d.c. potential was imposed. The similarity in magnitude between  $|Z|_{in}$  and  $R_n$  is interesting and is consistent with past work of this lab. The similarity between the  $|Z|_{in}$  and  $R_n$  trends supported the use of the sensors as monitoring devices for both EIS and ENM experiments. The deterioration of the Air Force coating during the ac-dc-ac testing as observed in the EIS data was also observed in the ENM data.

The noise resistance  $R_n$  values are given as functions of immersion time in Fig. 9(a) for the Army coatings together with the  $|Z|_{in}$  associated with these coatings. The  $R_n$  values remained approximately constant at  $7 \times 10^8$   $\Omega\text{ cm}^2$  up to 102<sup>nd</sup> day of immersion. This was consistent

with the trend observed for the  $|Z|_{in}$  values. After the application of the  $-8$  V d.c. potential for 8 hours the  $R_n$  value dropped to  $10^6 \Omega \text{ cm}^2$ . This significant decrease paralleled the decrease observed in EIS  $|Z|_{in}$  values.

#### 4. Conclusions

The consistency among the different sensor measurements demonstrated the reliability of the sensors as *in-situ* monitoring devices. The experiments conducted were intended to demonstrate the capability of these embedded sensors to monitor the coating degradation that is induced by the ac-dc-ac test protocol. The decrease in the  $|Z|_{in}$  values associated with the coatings demonstrated that the sensors were able to detect changes associated with the primer/ metal interface. The analysis of the EIS data by an equivalent circuit model provided a more detailed examination of the barrier characteristics of the primer/substrate systems. It was assumed that the resistance of adhesion layer was related to the strength of adhesion between the primer and the substrate. The data from the control samples indicated that continuous immersion in 3.5 wt.% NaCl did not diminish this adhesion property provided by the primers for up to 110 days of immersion. The data presented indicated that anti corrosive properties of the Air Force primer maintained themselves after being subjected to  $-4$  V d.c with delamination being assumed based on the reduced adhesion layer resistance. However, the anti corrosive properties of the Army primer were apparently irreversibly degraded after a  $-8$  V d.c. 8 hour application with both the charge transfer resistance and the adhesion resistance dropping by an order of magnitude off indicating increased corrosion and delamination. The evolution of the  $|Z(\text{low } f)|$  parameters obtained from the EIS data was consistent with the noise resistance parameters for both systems.

#### Acknowledgments

This work was supported by the Army Research Laboratory, Contract No. W911NF-04-2-0029 and the Air Force Office of Scientific Research under Grant No. FA9550-04-1-0368.

#### References

1. G. Koch, M. Brongers, N. Thompson, Y. Virmani, and J. Payer, *Corrosion Cost and Preventive Strategies in the*

- United State*, Technical report, CC Technologies Laboratories and NACE International, Dublin, OH and Houston, TX (2001).
2. T.C. Simpson, P.J. Moran, W.C. Moshier, G.D. Davis, B.A. Shaw, C.O. Arah, *J. Electrochem. Soc.*, **13**, 2761 (1989).
3. T. C. Simpson, P. J. Moran, H. Hampel, G.D. davis, B.A. Shaw, C. O. Arah, T.L. Fritz, Ken Zankel, *Corrosion*, **4**, 331 (1990).
4. T.C. Simpson et al., *Corrosion Testing and Evaluation: Silver Anniversary Volum*, ASTM STP 1000, ASTM, 397, Philadelphia (1990).
5. G.D. Davis, C.M. Dacres, M. Shook, B.S. Wenner, *Proc. of the Intelligent NDE Sciences for Aging and Futuristic Aircraft*, p. 41, El Paso (1998)
6. G.D. Davis, C.M. Dacres, L.A. Krebs, *Proc. of the 1999 Tri services Conference on Corrosion*, Myrtle Beach (1999).
7. G.D. Davis, C.M. Dacres, et al., *Mater. Perform.*, **3**, 46 (2000).
8. G.P. Bierwagen, X. Wang, D.E. Tallman, *Prog. Org. Coat.*, **4**, 163 (2003).
9. J. Kittel, N. Celati, M. Keddum, H. Takenouti, *Prog. Org. Coat.*, **4**, 93 (2001).
10. J. Kittel, N. Celati, M. Keddum, H. Takenouti, *Prog. Org. Coat.*, **4**, 135 (2003).
11. A. Miszyk, T. Schauer, *Prog. Org. Coat.*, **5**, 298 (2005).
12. K. N. Allahar, Quan Su, G. P. Bierwagen, D. Battocchi, V. J. Gelling, D.E. Tallma, *Proc. of the 2005 Tri services Corrosion Conferenc*, Orlando (2005)
13. K. Allahar, Quan Su, G. Bierwagen, D. Battocchi, V. Johnson Gelling, D. Tallman, *Proc. of NACE Corrosion/2006 Conferenc*, San Diego (2006).
14. J. Hollaender, E. Ludwig, S. Hillebrand, *Proc. of the Fifth International Tinplate Conferenc*, p. 300, London, (1992)
15. J. Hollaender, *Food Additives and Contaminants*, **146**, 617 (1997).
16. M. T. Rodriguez, J.J. Gracenea, S.J. Garcia, J.J. Saura and J.J. Sua, *Prog. Org. Coat.*, **5**, 123 (2004).
17. M. Bethencourt, F. J. Botana, M. J. Cano, R. M. Osuna, M. Marcos, *Prog. Org.Coat.*, **4**, 275 (2004).
18. M. Poleman, M. G. Olivier, N. Gayarre, and J. P. Petitjean, *Prog. Org. Coat.*, **5**, 55 (2005)
19. G.J. Fleer, MA.Cohen Stuart, J.M.H.M.Scheutjens, T. Cosgrove and B. Vincent, *Polymers at Interface*, Chapman and Hall, London (1993)
20. K.A.Dill & S. Bromberg, *Molecular Driving Forces*, p. 629, Garland Science, New York, 2003.
21. W. H. Press, S. A. Teukolsky, W. T. Vetterling, and B. P. Flannery, *Numerical Recipes in Fortran 77*, 2nd edition, p 402, Press Syndicate of the University of Cambridge, Cambridge (1992).